UNIVERSITY OF CALIFORNIA,
IRVINE

Linear Polyethylenimine Self-Assembly Polymer as a Nanopatterning Template to Prevent Bacteria Adhesion and Biofilm Formation

THESIS

Submitted in partial satisfaction of the requirements
for the degree of

MASTER OF SCIENCE

in Materials Science and Engineering

by

Christie Sutanto

Thesis Committee:
Professor Albert Fan Yee, Chair
Professor Regina Ragan
Professor Ralph VV. Clayman, MD

2018

TABLE OF CONTENTS

LIST OF FIGURES

ACKNOWLEDGMENTS

I would like to express my greatest gratitude to my advisor, Professor Albert F. Yee at the University of California Irvine, for you provided me with the practical and moral supports throughout my project and beyond. Thank you for believing in my research and the financial supports I received. Thank you for giving me so much direction and answering all of my questions. I appreciate every innovative ideas, feedbacks, and critiques you gave me. Thank you for being an amazing advisor, mentor, researcher, and instructor!

I would like to thank my committee, Prof. Regina Ragan and Dr. Ralph VV. Clayman, MD, and postdoctoral fellow, Dr. Ming Yang, for numerous discussion and feedbacks. To Prof. Michelle Khine who supported this project by providing the laboratory space and equipment. To Dr. Qiyin Li for the instrumentation training and guidance. To my fellow graduate student, Sara E. Heedy, for helping me get my start with my research and for critical reading and helpful comments for this thesis revision, Rachel Rosenzweig for her assistance on bacteria and fungi study. To Yee's family: Junming Cai, Xin Fu, Van Ly, Sydney, Yuhang Cai, and Emma Mah for their valuable suggestions and comments in every phase of this research.

Finally, thank you for my mom, Lina I. Agoes, for her love and support. Thank you for my sister who always lending me her ear and giving me advice. To Tamanna Khandaker, for being my best friend and my companion, for challenging me and bring me out of my comfort zone. This thesis is dedicated to all of you.

This research is supported partially by CDMRP grant W81XWH-17-1-0355 and the National Science Foundation (NSF) Innovation Corps program.

ABSTRACT

Linear Polyethylenimine Self-Assembly Polymer as a Nanopatterning Template to Prevent Bacteria Adhesion and Biofilm Formation

By

Christie Sutanto

Master of Materials Science and Engineering

University of California, Irvine, 2018

Professor Albert F. Yee, Chair

In the USA, yearly, over 1.7 million patients acquire infection during their hospital stay; about 99,000 of them died. The only cure and prevention currently in use are antibiotics; however, more severe infections have been seen in the past decade because of the development of microbial resistance to antibiotics. We have discovered that it is possible to engineer a nanopatterned surface that can kill and/or prevent the growth of microbes by mimicking nature's antibacterial surfaces. Others have explored top-down approaches, such as lithography and anodization to fabricate an array of nanopatterned surfaces. Limitations for such an approach are the size of the template and types of surfaces. Here, I describe the use of a self-assembled microstructured polymeric surface coating that is inherently biocompatible and designed to overcome the problems described above. The desired surface is coated with LPEI (linear polyethylenimine), a hydrogel that undergoes water-induced crystallization. By controlling the solution pH and concentration, the simple dip-coating method can be used to fabricate coatings with nanostructure possessing well-defined morphology and tunable geometry on any arbitrary surface. Using material characterization techniques and rheometer, an insight to LPEI macromolecules behavior in the solution to promote pillar-like morphology formation can be

described. Specifically, I focused on gaining an understanding of the effect of the cohesive behavior of LPEI macromolecules and the interaction of the polymer with water in controlling such morphology. Our grand vision is to be able to engineer an effective, long-lasting, and biocompatible coating layer to prevent device-associated infection around the world.

1. Introduction

Catheter associated urinary tract infections (CAUTIs) are the fourth most common types of infections developed in the hospital; they account for 12 percent of cases reported by the Centers for Disease Control and Prevention (CDC).[1,2] The cost of medicating these infections has reached $250 million per year in 2015, owing to the longer hospitalization and increased antibiotic doses required.[3] Our case study, supported by the National Science Foundation (NSF) Innovation-Corps program, further points to the facts that CAUTIs can increase medical costs by prolonging the hospital stays for an average of 8 extra days. Failing to treat the infection can lead to the spreading of the bacteria to the kidney and eventually to the bloodstream. It can cause kidney infection (pyelonephritis), blood poisoning (urosepsis) and, in extreme cases, death.[2,4,5]

Several improvements to catheter care have been made to reduce the rate of CAUTI. These improvements include betadine swabbing of the genital area twice a day, urine volume monitoring, antibiotic intake, and replacement of the catheter every 3-5days. Despite keen attention paid by hospitals to prevent CAUTIs in catheterized patients, the risk seems to be unavoidable. A study by Tsuchida *et al*. assessing the risk of CAUTIs suggests that improved catheter care could reduce only 50 percent of the risk.[6] The reason is that most of these infections are caused by the drug resistant-bacteria, which is difficult to treat, thus the catheter surface provides an ideal surface for these bacteria to adhere and to develop into biofilm.[7] Confronted by this challenge, research toward antibacterial surfaces to reduce the risk of CAUTIs without the use of antibiotics or drugs is highly desirable.

In this thesis, a pillar-like surface coating with antimicrobial property for indwelling catheters is developed. This surface-structured design circumvents the global problem of antibiotic resistance; it also prevents the growth of bacterial infections, regardless of their

morphology and biochemistry. Two criteria need to be considered in developing such surface coating. First, the material should be compatible with the human body. The material should not trigger any inflammatory response, should provide comfort and allow easy insertion through the urethra. Linear polyethylenimine (LPEI) is a suitable material as it is a hydrophilic polymer and is used extensively in drug-delivery applications.[8–10] It has also been found that linear polyethylenimine exhibits antimicrobial properties.[11,12] Second, the coating process must be industrially scalable and offer good control to achieve the desired structure that can be integrated to the existing catheter production line and eventually lead to the successful commercialization of this technology.

Therefore, the goal of this research is to create a coating layer of LPEI polymer on the surface of urinary catheter with tunable morphology through a simple and scalable dip-coating method. In particular, an in-depth understanding of LPEI macromolecular configuration in relation to the morphology of the coating layer on catheter surfaces was investigated. The rest of the paper is organized as follows: Literature review on antimicrobial coating agents for urinary catheters and materials selection and justification are discussed in chapter 1. Surface treatment process and its influence on the adhesion of LPEI coating layer are described in chapter 2. The influence of LPEI macromolecular configuration in solution on the coating layer morphology are examined in chapter 3. The limitations of the study are discussed in chapter 4. Lastly, future work is outlined in chapter 5.

1.1 Antimicrobial Coatings for Urinary Catheter

1.1.1 Urinary catheter: CAUTI, problem of long-term catheterization

Urethral catheterization is a common medical procedure to drain urine for pre/intra/post-operative patients who experience urinary retention and/or urinary incontinence. As the time of

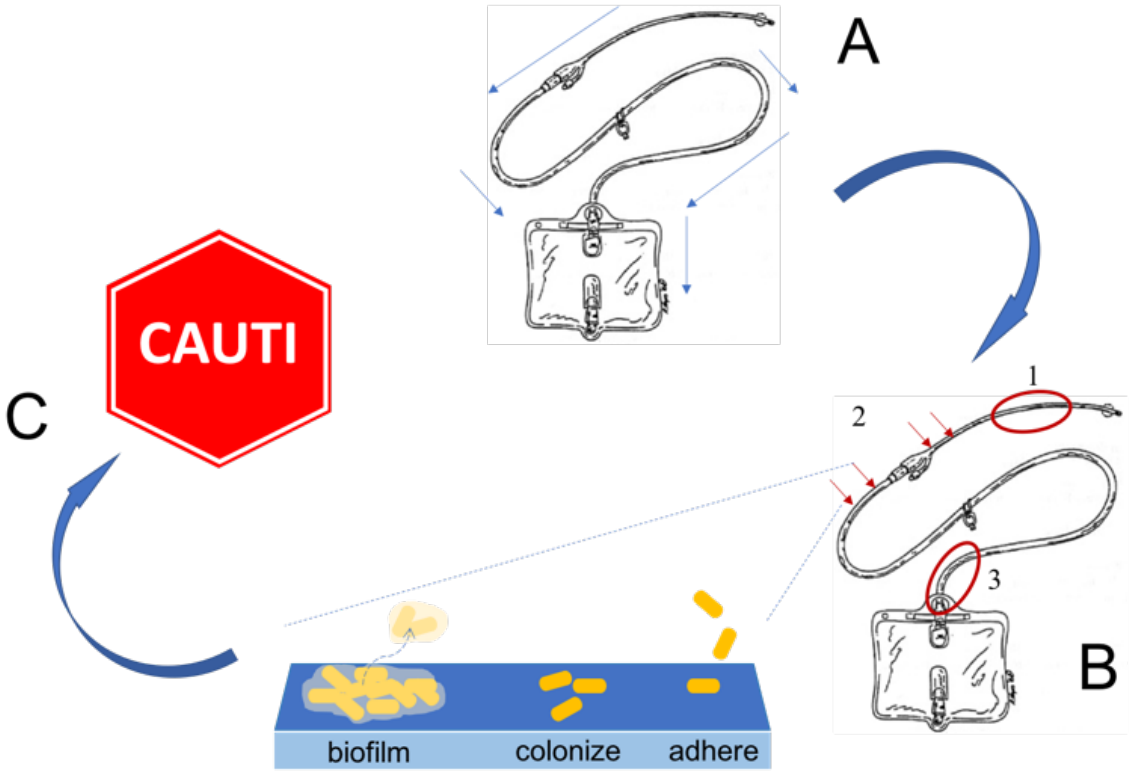

Figure 1. Schematic diagram of the cause of CAUTI in long-term catheterization

catheterization is varied depending on patient conditions, for long-term use, a Foley catheter (see figure 1A) attached to a drainage bag is most commonly prescribed. The catheter consists of the head or tip, drainage tube, and collection bag. The application procedure involves insertion of the tip and tube from the urethra until urine flows. The small balloon near the tip is inflated to hold the tip inside the bladder. The urine flows freely to the collection bag that is positioned lower than the urethra. Although these types of catheters are usually for short-term use in patients, many use it for a few weeks to months.[13] Due to the prolonged use of catheters, patients are at

risk of biofilm formation leading to infection.[14–16] It has been reported that all patients who undergo long-term catheterization developed CAUTI.[5]

Bacteria come into contact with the surface of urinary catheters in two different ways: extraluminal and intraluminal. In general, bacteria gain entrance to the bladder interluminally from the contaminated collection bag or the drainage tube junction (see figure 1B.2, 1B.3),[17–19] and extraluminally from the colonized urethral meatus as depicted in figure 1B.1.[20,21] For a closed-system, as in Foley catheter, the extraluminal route becomes more important in the development of bacteriuria. By employing animals in a short-term catheter use (8 days period), researchers demonstrated the migration of mixed bacteria from the outside of tubing into the meatus-urethra interface to the bladder. Within 72 to 168 hours from the initiation of this process, biofilm is formed in the bladder.[22,23] In addition to biofilm formation, some bacteria (urease-positive pathogens) can cause encrustation or blockage of the bladder hole by the deposition of crystalline biofilm. These bacteria are capable of secreting urease, an enzyme to hydrolyze urea into carbamate and ammonia. The increase of ammonia concentration in urine increases the pH. As a result, calcium and manganese precipitate out and are deposited onto catheter surface.[24] Biofilm and encrustation are, therefore, the major problems for a long-term use urinary catheter.

1.1.2 Effort to Prevent Bacterial Adhesion and Biofilm Formation

Considering bacterial adhesion as a first step of biofilm formation and encrustation, many studies focus on designing an antiadhesive surface against invading bacteria. These include intrinsically antimicrobial coating,[25–27] polymer brushes,[28,29], hydrophobic/hydrophilic surfaces,[30] and charged polymers.[31] Antimicrobial agents, such as silver nanoparticles and nitrofural antibiotic have been commercialized as a coating film for urinary catheter to suppress bacterial

adhesion. The effectiveness of these agents in combating CAUTIs has been studie, although the evidence is inconclusive. While one study shows higher efficiency for the antibiotic nitrofural in combating CAUTIs,[32] another showed silver hydrogel as a better antimicrobial agent for such infections.[33] Indeed, the CDC has proposed further research on the effectiveness of antimicrobial catheters [34]. History has shown that *Eschericia coli* (*E. coli*) developed resistant to silver ions in 1969 [35], and again in 2015 by rapid evolution to constant exposure of silver nanoparticles and silver nitrate (after 225 generation) [36]. Bacteria adapts to its environment and evolves like any other organism. When inaccurate doses or inappropriate antimicrobial/antibiotic is prescribed, it gives a chance for bacteria to develop resistance to them. Hence, extra care must be taken in designing antimicrobial/antibiotic coating before its implementation to the device.

Another effort in preventing bacteria adhesion involves modification of surface chemistry and surface morphology/topography. Bacterial adhesion on the surface can be driven by Van der Waals forces, hydrogen bonding, hydrophobic/hydrophilic interactions, or electrostatic interactions, with an increasing attraction force as they approach the surface.[37] Chemical strategy to weaken these interactions are thus dependent on the hydrophobicity/hydrophilicity and surface charge of the material and bacteria cell wall. For example, a bacteria adhesion study involving a model surface with controlled hydrophobicity/hydrophilicity was conducted on self-assembled monolayers (SAMs)[38]. The SAMs functionalized with hydrophilic moieties such as hydroxyl and amine group are found to have greater effect in reducing bacterial adhesion compared to hydrophobic functionalized SAMs with methyl group on the surface [39–41]. Other hydrophilic coatings, such as polydopamine peptide (having catechol and amine group on the surface), have shown resistance to *Escherichia coli*, *Pseudomonas aeruginosa*, and *Staphylococcus aureus* [15]. However, the attachment of bacteria on surfaces is rather complex. It is observed that bacteria

adhere on hydrophilic surfaces more commonly than hydrophobic surfaces when the bacteria is surrounded by lower surface tension liquid, and vice versa [42]. A study on hydrogels with anti-adhesive hyaluronic acid additives shows an increase in biofilm formation by increasing the cell-cell interactions [43]. Although hydrophilic surfaces provide an anti-fouling surface to reduce bacteria adhesion, this surface characteristic by itself cannot effectively combat bacteria adhesion, nor biofilm formation.

Besides surface hydrophobicity, modification to have a charged surface has also been studied. The idea comes from the fact that bacterial cell wall mostly carries a net negative charge; therefore, bacteria will not adhere to the negatively charged surfaces and will not form a biofilm. Interestingly, study by Bart *et al*. to compare the antimicrobial effect of surface charges on gram-positive and gram-negative bacteria reported that positively charged surfaces exert higher antimicrobial effect compared to the negatively charged surfaces [44]. Notice that the positively charged polymer used in the study is poly(methacrylate)/ trimethylaminoethyl methacrylate-HCl salt (PMMA/TMAEMA-Cl) that carries negative ion chlorine. Chlorine ions are inherently antimicrobial. They inhibit the enzymatic/metabolic process of the cell, resulting in cell lysis [45]. In this case, bias was introduced to the material selection and thus the conclusion was not strongly supported. Besides, the gram-positive bacteria were able to survive despite a higher bactericidal activity on the positively charged surface. A similar study conducted by Terada *et al*. supported the idea that decreased adhesion can occur due to repulsion between the bacteria cell wall and the negatively charged surface. The negatively charged surface had less bacterial adherence and the positively charged surface had a strong electrostatic attraction that promoted bacterial adhesion. [46] Yet, biofilm formation was rapid on both surfaces. Adhesion is the first step for biofilm formation; the adhering bacteria needs to grow to fully developed

biofilm. [47,48] The surface design is, therefore, important to not only preventing adhesion but also inhibiting or killing any adhering bacteria.

1.1.3 Micro-structured coating in urinary catheter

The use of surface topography has benefits compared to antibiotic and antiadhesive coatings, because if topography could prevent the adhesion and the growth of bacteria, regardless of the morphology and biochemistry of the bacteria, then we would have a solution that has very broad application. This surface-structured design would also prevent bacteria adhesion by decreasing the contact area between the surface and the bacterium. The effectiveness of this surface topography, however, relies on the geometry and dimension of the structure.

Many studies on surface topography are inspired by unique surfaces found in nature. These surfaces include shark skin, lotus leaf, and cicada wings. With topographical features of micro- to nano-scales, these surfaces offer promise to control bacteria adhesion. Researchers, therefore, have studied their use as antifouling structured materials. The micron sized features such as sharklet pattern has been tested against *S. aureus* and *S. epidermidis*.[49] The bacteria are shielded from each other by the trenches formed by the protruding features, possibly preventing the formation of bacterial biofilms on the surface. Xu and Siedlecki further reported that the efficiency of surface pattern to prevent microbial adhesion depends on the size and geometry of the structure.[50] Recently, after the discovery of much smaller, nanostructured pillars on cicada wings, researchers realized the ability of surface topography to actually kill bacteria. Studies on nanostructured pillar arrays were then focused on designing such surfaces. For example, the study of nanoprotrusion of black silicon to mimic the dragonfly wings surface features against gram-positive and gram-negative bacteria and endospores.[51] The mechanical bactericidal effect showed surface topography is independent to chemical composition of the surface.[52] The killing

rate approached 450,000 cells min^{-1} cm^{-2} due to the high surface density of the pillars, which spacing is ranging from 20- 80nm. Depending on the application, the incompatibility of black silicon surface with eukaryotic cell may not be appropriate for implantable devices. The rigidity and brittleness of black silicon is another serious limitation. A more rigorous study was conducted by Dickson *et al.,* where the optimum pillar geometry was established by comparing difference sizes and periodicities of the pillar geometry. It was concluded that the pillar geometry of spacing between 130- 380nm efficiently killed the bacteria by triggering significant shape deformation (e.g. elongation and deflation) in response to a high stress nanopillar environment [53]. It is on the basis of her extensive study that I modeled the surface topography of the polymer coating on urinary catheter devices. This study differs from Dickson et al. in that I utilize a bottom-up approach in fabricating the nanostructure, therefore it is not restricted by the template size and has the capability for large-scale area processing. However, a bottom-up approach presents its own challenges, which I describe below, along with the solution I found.

1.2 Linear Polyethylenimine as Biomedical Coating of Urinary Catheter

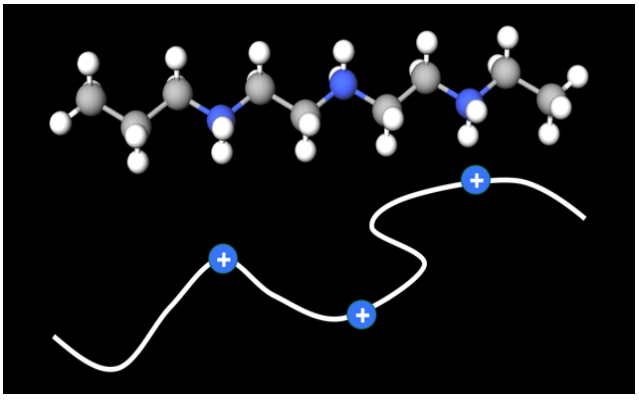

Figure 2. Molecular and schematic drawing of Linear Polyethylenimine (LPEI) polymer

The bottom-up method of nanostructure fabrication involves the use of building blocks (*e.g.,* atoms, molecules) to create the nanostructure. This approach is often limited by poor control over the spatial geometry.[54] Linear polyethylenimine (LPEI) is a cationic polymer, with cationic moieties along the chain as shown (*in blue*) in figure 2. It is also

a thermo-reversible hydrogel with hierarchical morphology. Recently, LPEI was used to direct biosilification of polysilsesquioxanes (PSQ) into well-controlled nanofilaments of 200nm in diameter which otherwise would form a mixture of incomplete cages, ladder-like, and network structures.[55] It was reported that biosilification occurred selectively on the LPEI substrate to form a coating layer, such that LPEI was a template for causing the nanofilament morphology. The structure-directing role of LPEI is again reported to improve the titanium dioxide network,[56] surpassing the previously reported by Carlos *et al*., which was directed by poly-L-Lysine and a polymer template.[57] Seeing the robustness of LPEI as a template for many inorganic substances, we are interested to adopt LPEI as a building block for forming the desired nanopillars. Besides, LPEI has shown potential as a disinfectant [58] and as a non-viral agent for drug delivery systems [59,60]. Unlike antibiotics, disinfectants do not require a specific binding site as part of their antimicrobial mechanism, consequently there is relatively less potential for bacteria and microbes to develop resistance to such antimicrobials. There have only been a few reports indicating the development of antimicrobial resistance against cationic disinfectant such as antimicrobial peptides (AMP) [61] and cationic methacrylate.[62] LPEI has also shown to increase the transfection efficiency of DNA and improve cell viability, irrespective of the physiological conditions [63]. Therefore, LPEI is chosen also for its biocompatibility and lower potential for microbial resistance development.

1.3 Chapter 1 Summary

Healthcare providers are challenged to reduce the risk of CAUTI because it prolongs the hospitalization time, increases antibiotic usage for patient, not to mention the possibility of kidney failure and blood poisoning. It is the background and motivation of my study to improve

patient safety by eliminating bacterial adherence and biofilm formation leads to CAUTI. A detail literature review on antimicrobial coating agents of urinary catheters, material and coating method selection were discussed in this chapter. I addressed the successes and drawbacks of antibiotic and antiadhesive coatings in preventing bacterial infection, explicating my choice of surface nanopatterning approach. Lastly, linear polyethylenimine usage as the coating material to fabricate the antimicrobial catheter was introduced. We believe that the use of LPEI as the material to form pillar-like structure can address the challenges in increasing number of microbial resistant to antibiotic and processing limitation of lithography method as mentioned above.

2. Surface Treatment of Thermoplastic Polyurethane with Oxygen Plasma to Improve Adhesion to LPEI

Catheters are often made from latex rubber, silicone rubber, and polyurethane. The LPEI coating is to be applied over a catheter made from one of these polymers. I chose (PU) based catheter for this study because PU is extensively used in other medical devices, such as artificial heart valves, dialysis cartridges, wound dressing, and short-term implants. In another word, successful incorporation of LPEI coating on PU material will have a significant impact on reducing microbial infection in many medical devices. In addition, PU can be crosslinked or thermoplastic. The material we choose in this work is a commercial tubing made from a thermoplastic PU. Thermoplastic PU is composed of soft molecular blocks and hard molecular blocks that are bound together via urethane linkages. In general, the soft blocks give PU the elasticity and the hard blocks give the rigidity. By varying the ratio, structure, and/or molecular weight of the hard and soft blocks, a broad range of thermoplastic PU's with different properties can be produced. In order to obtain a durable and continuous coating of LPEI on the surface of PU, it is important to have mutual surface compatibility between these two components. Flexibility to adjust parameters such as glass transition temperature and Poisson's ratio of PU material will be beneficial because differences in thermal expansion coefficients can induce thermal mismatch strains that result in cracking or delamination, especially when the coating process involves dipping of the substrate into a hot solution.

2.1 Superthane® Ether-Based Tubing for Polyurethane Stent Substitution

The commercial thermoplastic polyurethane used throughout this study is Superthane® ether-based polyurethane, purchased from the United States Plastics Corporation, Cat. No. 56407. We substituted the medical PU stent with commercialized PU because we aimed to monitor the microbial viability on the surface under inverted light microscopy. We can image live/dead cell by doping the microbial with fluorescent molecules. These molecules bind to the fluorescent light that passes through the sample during the imaging process. Considering this, the opacity of medical PU stent, as it can be seen in figure 3, makes it impossible to be imaged using this technique.

To gain confidence that the result obtained from commercial PU coated with LPEI will be translatable to medical grade PU stents, characterization of the commercialized PU was conducted using Fourier Transform Infrared Spectroscopy (FTIR). The comparison of FTIR spectra between commercialized PU and the medical grade PU stent allows us to validate their chemical structure. Similar to medical grade polyurethane, commercial PU is composed of soft blocks of polyether and hard blocks of aromatic based diisocyanate bonded together by urethane linkages. In figure 3, the molecular structure is shown and major peaks corresponding to the amine group and carbonyl stretching are highlighted. It is important to note that the urea (NHCO) and urethane (NHCOO) peaks appeared as merged peaks because their energy levels are close to each other. Due to the more electronegative environment of the urethane, the carbonyl group gives greater intensity to the IR stretching vibration which masks the presence of urea. Thus, the blue highlighted peaks in the FTIR spectra represent both the urea and urethane groups. These spectra demonstrate that the PU materials for the stent and the commercial tubing have the same molecular structure. This implies that commercialized PU is an appropriate

substitution for medical PU stents for the purpose of this study. I note that these two materials may have different molecular masses, a possibility that affects only the processability and mechanical modulus, and probably has no bearing on my study.

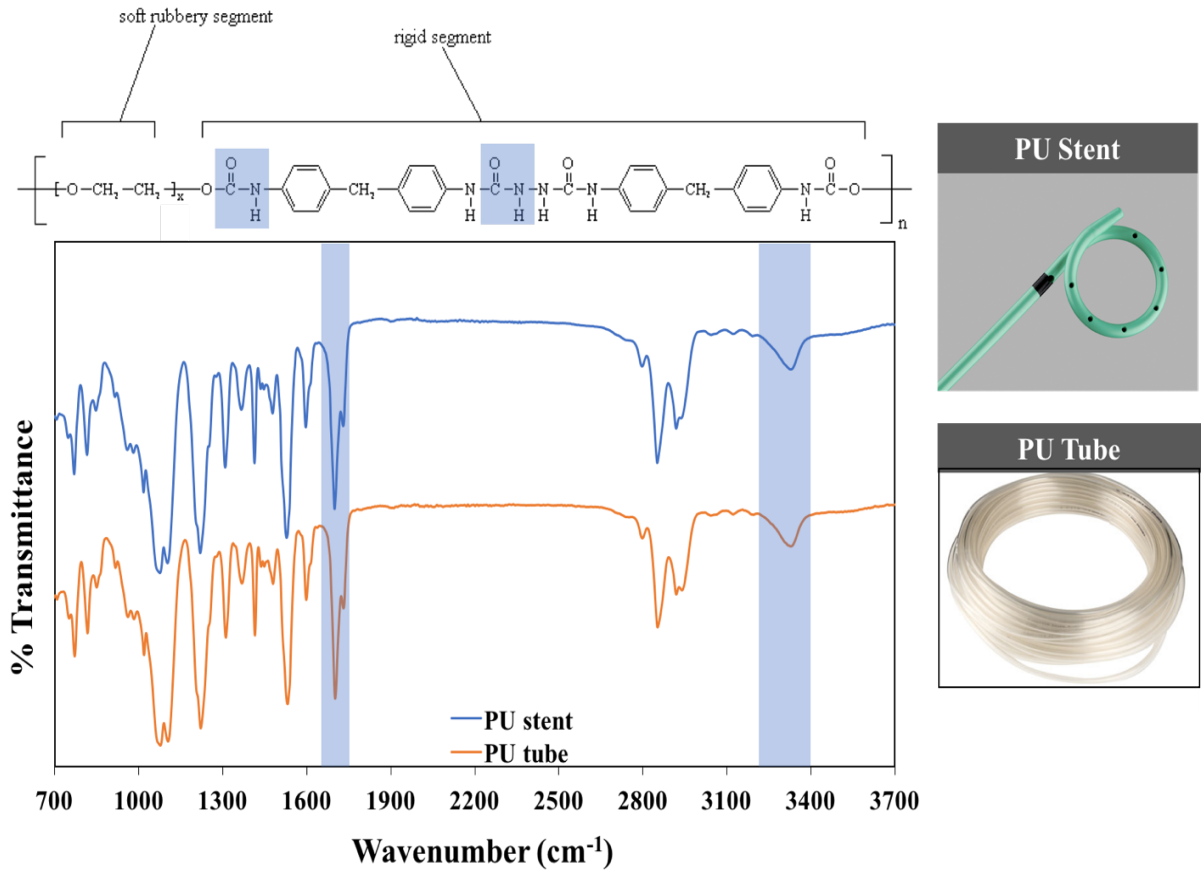

Figure 3. Comparison of FTIR spectra between PU-based catheter/PU stent and commercial PU/PU tube. A general polyurethane chemical structure is presented to indicate the functional groups present on both PU stent and PU tube. The ether group is shown in brown and urethane linkage in black and purple. Cited from Tips for Medical Device Tubing Selection. Med Des Briefs. 2014. http://www.medicaldesignbriefs.com/component/content/article/mdb/features/19236. Accessed November 27, 2016.

2.2 Influence of PU surface energy and interfaces

For all coating processes, a clean surface is critical to obtain better adhesion because the presence of contaminants prevents bonding between the coating material and the surface.

Equally important is for the surface to have a higher surface energy compared to the coating. This higher surface energy allows the coating materials to wet the surface area uniformly, and increases the binding forces. The thermoplastic PU tubing is inherently low in surface energy, making it difficult to bond with the coating layer. In the case of a catheter, even a small discontinuity on the coating could become a pathway for bacteria to adhere and grow into biofilm. For this reason, I activate the PU tubing surface with oxygen plasma. Plasma treatment using oxygen gas was used to firstly clean the PU tubing surface from organic contaminants that originate from the manufacturing process. Secondly, the excited oxygen plasma can interact with the surface, introducing a higher concentration of oxygen in the 1s electronic state and increasing the O 1s to C 1s ratio. [64] Details about the plasma treatment effect on the PU tubing surface is discussed later in this chapter. Nevertheless, the oxygen plasma activation did not weaken or discolor the PU tubing; it is non-toxic and non-hazardous and thus, a suitable surface treatment for medical devices.

2.2.1 Experimental details

The PU tubing was plasma treated using the Plasma Etch (PE-50) with frequency of 60 Hz. The oxygen supply gas was set to a flowrate of 7 cubic feet per minute (SCFM) to obtain the effective plasma generation. First, plasma chamber was flushed off with oxygen gas to remove the trace of nitrogen and other gases. The sample was then placed in the chamber and plasma treated for a given amount of time. Immediately after the sample was removed from the plasma chamber, contact angle measurement was performed using the sessile drop method with a Krüss D54305 goniometer. A droplet of 2µl DI water was formed on the tip of the syringe. Then, the droplet was deposited on the sample surface. All experiments were conducted at room temperature, 20 ˚C. The droplet contact angle analysis was carried using ImageJ software. Data

reported on the contact angle measurements were the average of 5 data points. The coating morphology after plasma treatment was analyze using XL-30 field emission scanning electron microscopy (FESEM) at an acceleration voltage of 10 keV, spot size of 3.0 nm, and working distance of 14.6 mm.

2.2.2 Results and discussion

Shown in figure 4 (top figure) is the graph of the PU tubing contact angle versus oxygen plasma treatment time. It is observed that the contact angle value of the plasma treated PU tubing decreases when the plasma time is increased. This is due to the oxygen radical reaction with the PU tubing surface producing isocyanate (N=C=O) groups on the surface. As depicted in figure 4, deprotonation of N-H (from the urethane group) by radical oxygen to form a double bond with the neighboring carbon. Therefore, additional overtone peaks at 2360 cm^{-1} corresponds to N=C=O symmetrical stretch and 2341 cm^{-1} for the asymmetrical stretch are observed. In the bottom figure, the PU tubing is seen to maintain its characteristic N-H stretch at ~3300 cm^{-1} and carbonyl at ~1700 cm^{-1} in the bulk material after the plasma treatment. The surface, however, undergoes deprotonation of N-H (from the urethane group) by radical oxygen to form a double bond with the neighboring carbon. Therefore, additional overtone peaks at 2360 cm^{-1} corresponds to N=C=O symmetrical stretch and 2341 cm^{-1} for the asymmetrical stretch are observed.

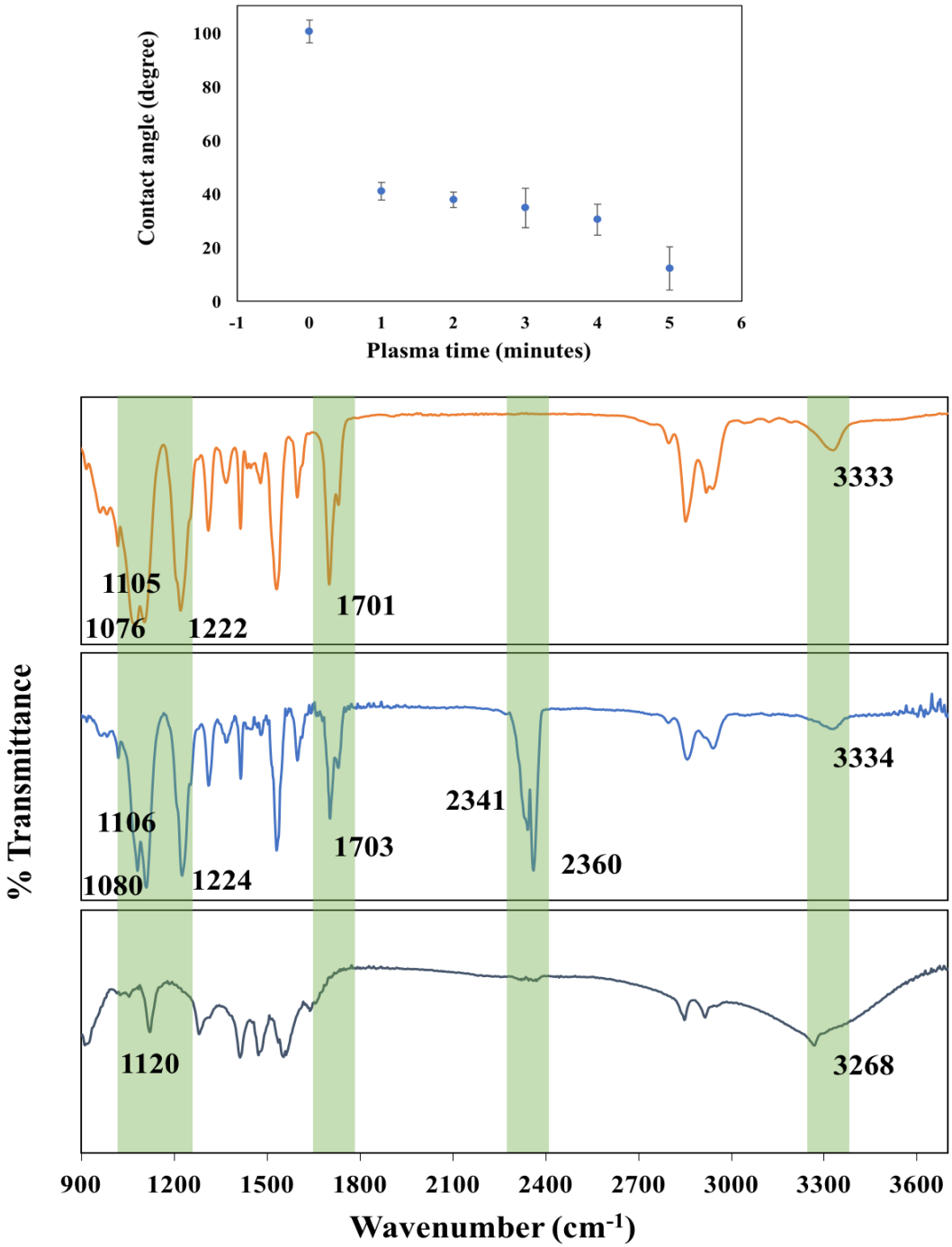

Figure 4. Top figure is the graph of the PU tubing contact angle value versus plasma treatment time. Bottom figure is the FTIR comparison of PU before plasma treatment, PU after plasma treatment, and LPEI coated PU.

At the time of coating, the isocyanate groups react with the amine of LPEI. In the last FTIR spectra in figure 4, the disappearance of isocyanate peaks is accompanied by the redshift of -NH stretch vibration and broadening of the peak at ~3300 cm^{-1}. This occurs as a result of extensive intermolecular hydrogen bonding between the amine group of LPEI and the carbon of isocyanate functional groups. In addition, LPEI also reacted with PU tubing surface through ester the group of urethane linkages. This reaction can be seen from the replacement of two strong absorption peaks in region 1000- 1300 cm^{-1} with single peak at 1120 cm^{-1}. The C=O of ester group causes the neighboring C-O to experience two vibration modes. After the C=O double bond reacts with amine of LPEI, the double bond was opened up to become C-O-H.[65] Thus, the single peak at 1120 cm^{-1} can be regarded as C-O stretch from urethane linkages alone.

It was also observed that the plasma treatment roughened the surface of PU tubing as it depicted in figure 5A. Surface roughness can play an important role in the adsorption of LPEI. Roughening the surface tends to improve the adhesion of polymer to the surface by increasing the surface area. However, it is important to note that the enhance adsorption arises from the enhance probability of polymer intersecting the rough surface and not so much about the increase area of the rough surface.[66] It implies that the dimension of the surface should be greater than the LPEI hydrodynamic volume to promote better adsorption. If the polymer is much larger than the rough surface dimension, it should lead to a diminished polymer-surface interaction. From figure 5B, I have found that when the PU tubing was pretreated with oxygen plasma for 2 min results in a homogenous deposition of LPEI, leading to fiber-web like morphology. As plasma treatment increased and the surface became more etched, LPEI coating gave a patchy morphology to the

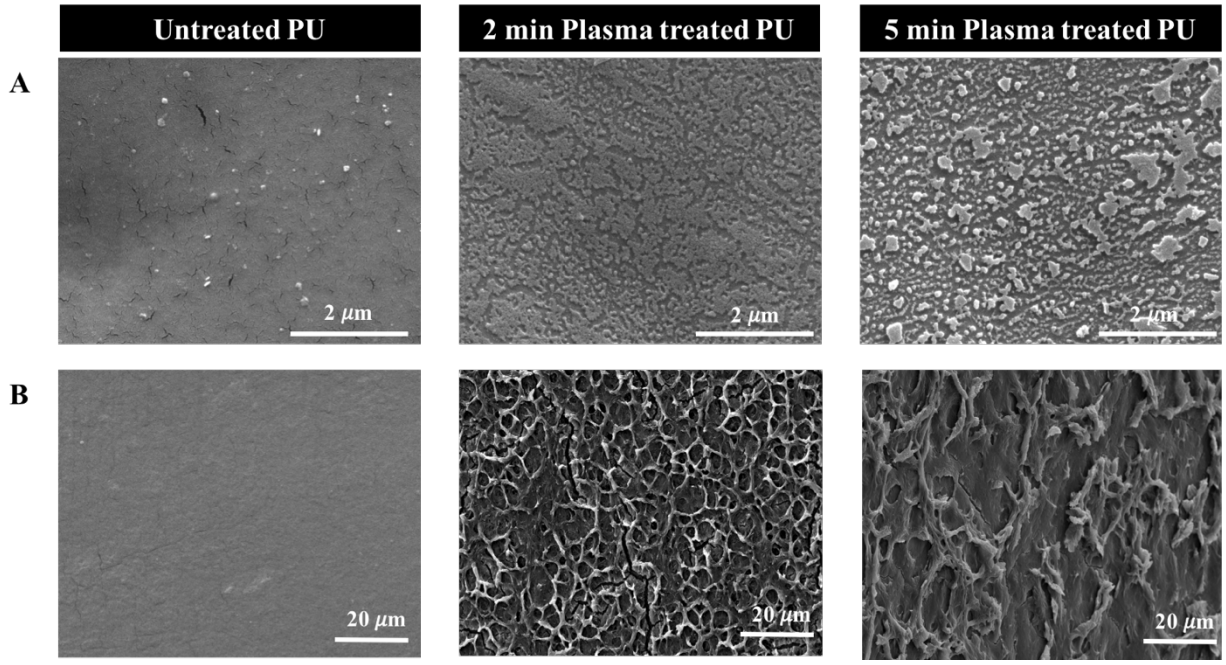

Figure 5. A) SEM images of PU tubing surface after plasma treatment. B) SEM images of PU tubing surface after LPEI coating

surface. Given this result, it was determined that 2 min of plasma treatment was the optimum time for LPEI deposition on PU tubing surface.

2.3 Chapter 2 Summary

In this chapter, a background on PU stent replacement with commercial PU was described. The PU stent has an opaque color. Considering the inverted microscopy that will be used to observed the bacteria and fungi grow, a substitution to a transparent PU tubing was made. I also discuss the influence of plasma treatment in increasing the PU tubing surface energy. The oxygen plasma pretreatment aims to increase the surface energy of the PU tubing so as to favor the interaction of functional groups to amine groups of LPEI. The functional groups that form from plasma treatment is identified as isocyanate group. From the FTIR spectra, it was found that this group and ester group are responsible for the binding between LPEI and PU tubing surface.

3. Polyurethane Surface Coating with Linear Polyethylenimine

LPEI has a unique macromolecule configuration in the solution as a result of the cationic amine groups along the chain. The lone pair in amine sp^3 hybridization makes amine act as a base as well as a nucleophile. This nucleophilic behavior causes amine to be easily protonated by water molecules. Although this protonation is stabilized by the ethylene groups along the chain

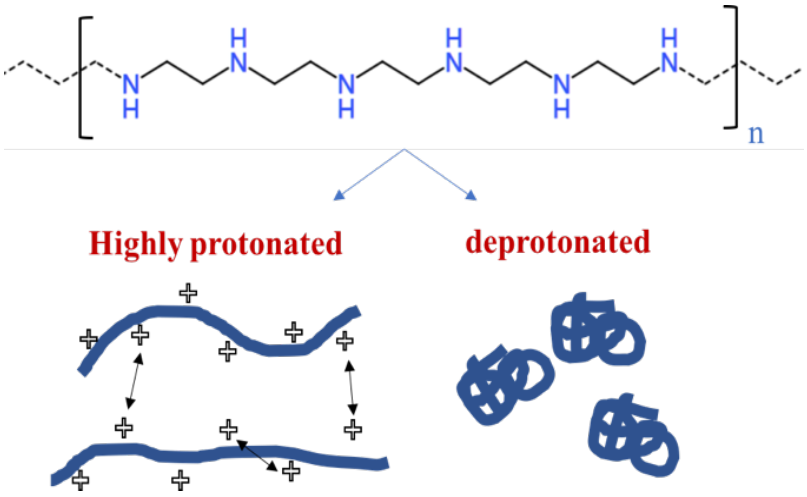

Figure 6. LPEI macromolecule configuration in the solution under two extreme conditions, highly protonated and deprotonated.

as it donates electrons, it is inherently unfavorable. Thus, a dynamic exchange of amine between the protonated and un-protonated states occurs. For this reason, the long chain LPEI adopts various configurations in the solution with the extremes being an extended chain and a highly coiled configuration. When there is sufficient charged amine in the chain, the repulsion force favors LPEI to adopt an extended chain configuration.[67] On the other hand, when the LPEI is dominated by the unprotonated state of amine, hydrophobic ethylene groups in the chain will minimize the interaction with water molecules by collapsing as highly coiled LPEI. [68]

As hydrogen bonding is the major intermolecular interaction between the LPEI and the PU tubing surface, the dynamic equilibrium of LPEI in the aqueous solution becomes important. The degree of LPEI coiling determines the availability of its amine groups to interact with the surface; in another word, adhesive interaction. Therefore, I varied the pH of LPEI solution to obtain the protonated/unprotonated LPEI macromolecules and relate this to the adhesion behavior and eventually the morphology of the coating layer.

3.1 The Influence of LPEI Chain Configuration to The Morphology of Coating Layer

3.1.1 Experimental details

The two extreme configurations of LPEI macromolecules were prepared by dissolving LPEI powder into two stock solutions, acidic and basic solution of pH 2 and 12, respectively. The LPEI used in our experiment was ~10,000 g/mol in molecular weight, purchased from Sigma Aldrich (lot# MKCC1827). Generally, LPEI solution with pH 2, 7, and 12 were made by dissolving the as-received LPEI powder into acid/basic stock solutions at ~80˚C. The acid stock solution was prepared by diluting concentrated hydrochloric acid solution (Fisher Scientific, 171924) of 12.1 M with miliQ water to final concentration of 0.01 M. The basic stock solution was prepared by dissolving sodium hydroxide pellets (Fisher Scientific, M-12676) with miliQ water to obtain 10^{-12} M aqueous solution. Hydrochloric acid and sodium hydroxide solutions were used to prepare the stock solutions as they do not react with LPEI. After the stock solutions were homogenously mixed, LPEI powder of 3wt% was added to the solution and continuously stirred at ~80˚C. The PU tubing was then dipped into the hot solution and withdrawn immediately. The sample was left to dry under ambient temperature and humidity. The surface morphology of LPEI coated PU was imaged using a XL-30 field emission scanning electron

microscopy (FESEM) at an acceleration voltage of 10 keV, spot size of 3.0 nm, and working distance of 14.6 mm.

3.1.2 Results and discussion

Our results showed that the two extreme configurations of LPEI, fully extended chain (pH=2) and highly coiled chain (pH=12), produced thin, translucent coatings, as depicted in figure 6A. Moreover, LPEI configuration at pH 7 produced a thicker coating. FESEM morphological analysis revealed that there was no microstructure development in thin coated samples, whereas a pyramid-like structure was observed on the thicker coated sample. This observation can be explained from the protonation/deprotonation behavior of amine under the acidic/basic environments, as shown in Fig. 5.

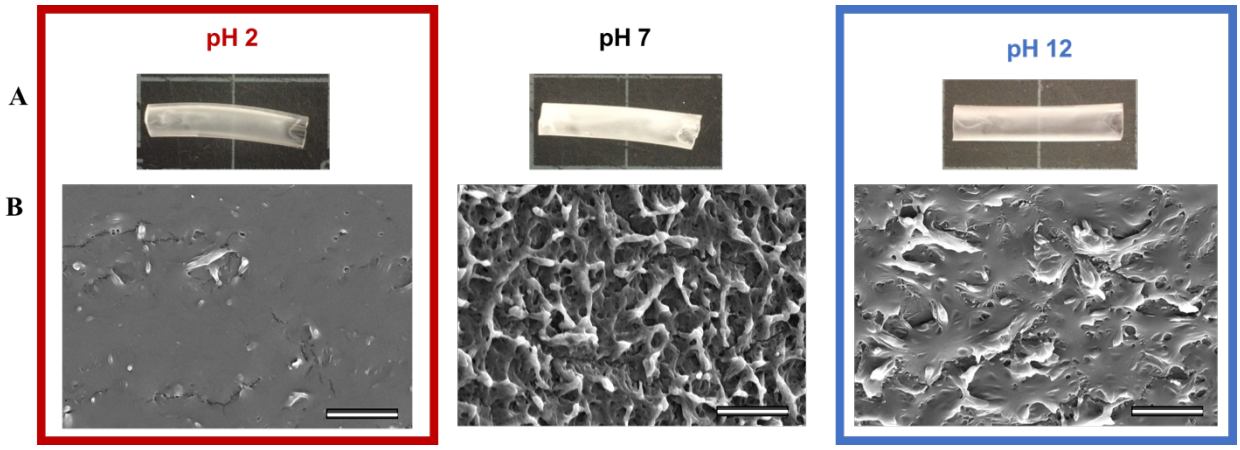

Figure 7. A) Photographic images of the LPEI coated PU tubing from different pH solution. B) SEM images of LPEI coated PU tubing surface morphology. Scale bar is 10μm.

The extended chain or highly coiled configuration of LPEI is determined by the amount of water molecules along the chain. The molecular dynamics study of LPEI by Roy *et al*. suggests that the amount of water along the LPEI chain increases from basic to acidic condition, transforming the highly coiled LPEI macromolecule to an extended chain configuration.[67] In basic condition, the free hydroxyl from the dissociation of sodium hydroxide tends to remove the

hydrogen from LPEI secondary amine and form water. As a result, LPEI becomes deprotonated and highly coiled. The reverse occurs by adding acid into the solution. The amine in LPEI becomes a stronger base and takes the excess of hydrogen atoms from acidic water molecules. The LPEI chain is elongated by the hydrogen bonded water molecules, adopting an extended chain configuration. The presence of water molecules along the chain of LPEI, thus, increases the dispersion of LPEI in the solution. The adsorbed water molecules can be regarded as a shield that inhibits interaction between LPEI chains. Similarly, the intermolecular interaction of LPEI is reduced when LPEI is suspended in the pH 12 stock solution. The reason is that the attraction between LPEI chains is due to Van der Waals forces, such as the hydrophobic interactions of the ethylene groups. The highly coiled configuration of LPEI does not provide enough binding area for these weak interactions to sustain. In both cases, as the polymer/polymer interaction was reduced, thin coating was obtained and the morphology of LPEI coating appeared "flat". At pH 7, where random protonation and deprotonation of amine by hydrogen atoms occurs, we argued that the solution will consists of a mixture of coiled and uncoiled macromolecules. The effect of LPEI random coiled configurations, in some way, might promote the polymer/polymer interaction that leads to the formation of "pyramid-like" microstructure. [69] This hypothesis was examined in the next chapter.

3.2 Influence of Solution Concentration on Morphology of Coating Layer

3.2.1 Experimental details

A given amount of LPEI and miliQ water were charged into a 20 ml vial to obtain 1, 2, 3, 4, and 6 wt% mixtures of pH 7. The mixture was heated to ~80 ˚C and continuously stirred until completely dissolved. The PU tubing was dip-coated into hot LPEI solution and dried under

ambient temperature (22 ˚C) and humidity (25% RH). The surface microstructure of LPEI coated PU was characterized using the XL-30 field emission scanning electron microscopy (FESEM) at the accelerating voltage of 10 keV, at 14.6 mm working distance and spot size of 3.0 nm. The sample was sputter coated with platinum/paladium for 4 nm thick. The LPEI viscosity as a function of weight fraction was measured using a rheometer from TA instrument (AR G2) with the cone and plate system. The cone was 40mm in diameter, with 60μm truncation, and 2˚ cone angle. The measurement was conducted under a constant frequency of 500 Hz and constant temperature (80 ˚C). The gap height was 20μm. The melting temperature of LPEI hydrogel was determined by using a heat-cool-heat cycle method of the differential scanning calorimetry (DSC) from TA Instrument, Q2000. 3wt% LPEI hydrogel of ~10 mg was hermetically sealed with aluminum pan and lid. A small hole was punched on the lid to allow water evaporation. Slow heating rate of 5 ˚C/min and fast cooling rate of 20 ˚C/min were used during the test. The sample was held isothermally at 200 ˚C for 1 minutes before the cooling run. Standard TGA test was performed using the TA Q500 instrument in the temperature range of 30- 500 ˚C and heating rate of 20 ˚C/min.

3.2.2 Results and discussion

In this section, we increased the polymer/polymer interaction by increasing the concentration of LPEI in the solution to then relate it to the surface morphology. Figure 7 shows the SEM images of LPEI coated PU tubing surface fabricated from different LPEI solution concentrations. In general, the aggregate morphology started to dominate as LPEI concentration was increased. At 1wt% of LPEI solution, thin fibrous bundles that lied flat on PU tubing surface were formed. These fibrous bundles consist of spherical aggregates in the center of its dendrites. The fibrous bundle diameter grew larger and eventually formed standing “pyramid-like”

structures when the LPEI concentration reached 3wt%. At 4wt%, the pyramid-like structures became denser, and covered the surface unevenly with aggregates. A completely different morphology was seen as LPEI concentration reached 6wt%.

As the LPEI concentration is increased, the mobility of the polymer molecules within the solution is restricted due to chain-chain interactions. In a dilute solution, where there are no effective polymer interactions, the relationship between viscosity and concentration is generally linear. At higher concentration, the polymer interactions in the solution cause the viscosity to depend on the concentration with an exponential of power law relationship[69] that is described by Martin equation:

$$\frac{\eta_{SP}}{C} = [\eta]\, exp(K_M[\eta]C)$$

where $\eta_{SP} = (\eta_r - 1)$

and Baker equation:

$$\eta_r = \left(1 + \frac{[\eta]C}{\eta}\right)^n$$

where $\eta_r = \frac{\eta}{\eta_0}$

The variables are listed as follows:

η_{SP} : reduced specific viscosity

η : viscosity of solution

η_0 : viscosity of solvent

η_r : relative viscosity

K_M : Martin's coefficient

C : concentration of solution

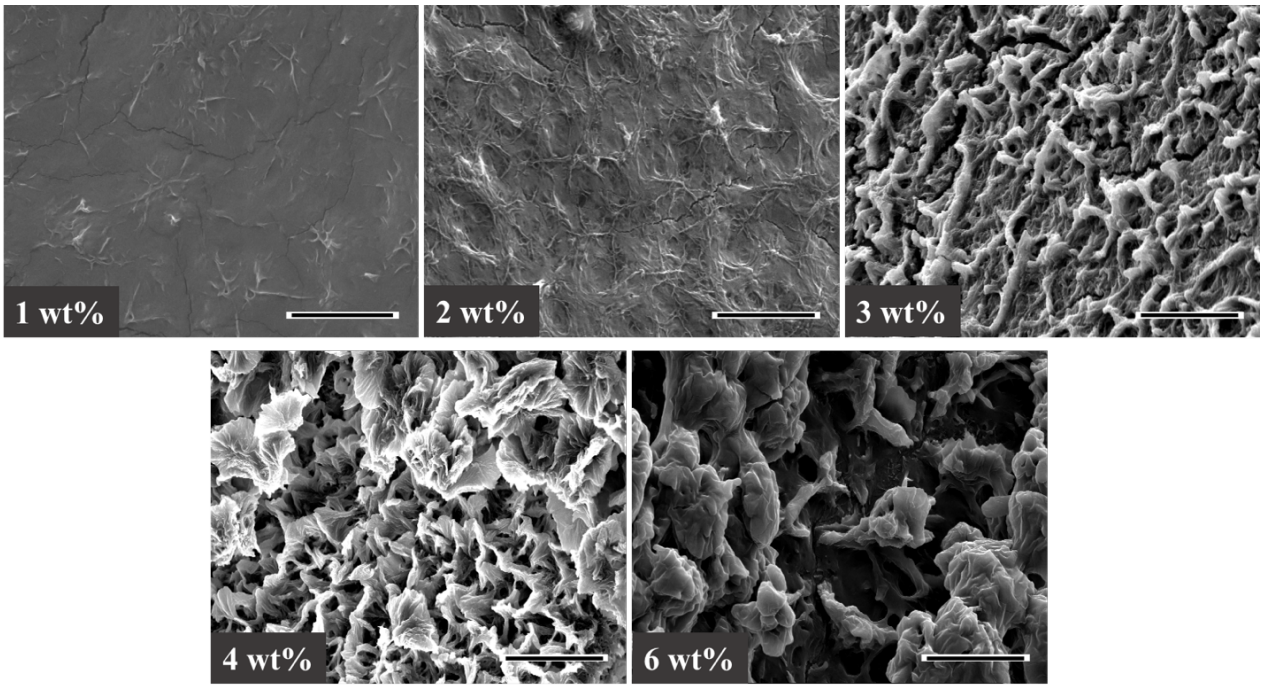

Figure 8. SEM images of LPEI coated PU tubing surface morphology that are fabricated from different LPEI solution concentration. Scale bar 10 μm.

Therefore, it is possible to determine whether increasing polymer concentration also means increasing the polymer/polymer interaction by plotting the viscosity versus concentration. In figure 8A, LPEI solution viscosity was plotted against its concentration in the solution. As expected, LPEI viscosity increased approximately linearly with the concentration and inflection point appeared at LPEI concentration of around 4.5 wt%. This result implies that the pyramid-like morphology at 3wt% does not originate from the overlapping of polymers in the solution. Considering LPEI densely packed cationic group, I conjecture that the viscosity increased might result from increasing LPEI interaction with water, affecting the morphology of the resulting gel structure. To further elucidate the interaction between LPEI and water molecules, the weight loss and melting point of 3wt% LPEI hydrogel was examined with TGA and DSC, respectively. From the TGA curve, I observed two major weight losses occurred in a temperature range of 25-110˚C and 110- 380˚C. The first weight loss of 96.31wt% was due to water evaporation and the

remaining 3.34 wt% was probably due to LPEI decomposition. This hypothesis was confirmed by performing DSC scan on the sample. From figure 8B, we observed a broad endothermic curve between 30 to 120 ˚C with a sharp peak at 104.7˚C as a result of the first DSC heating run. Upon hydration, hydrogel can interact with water molecules and coordinate them along the molecules

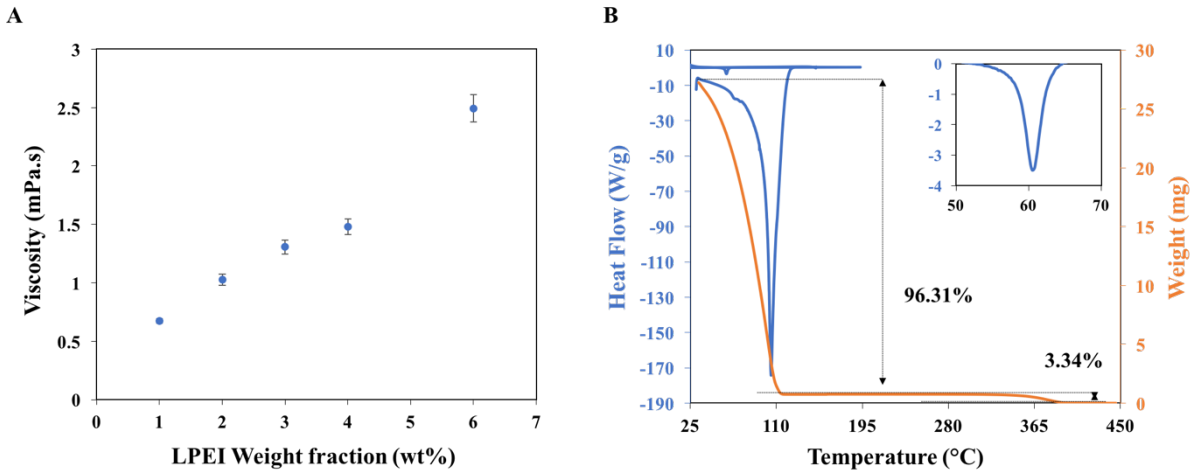

Figure 9. A) Graph of LPEI solution viscosity as a function of LPEI weight fraction increases linearly. B) TGA-DSC curve of 3wt% LPEI hydrogel water evaporation.

and also in the interstitial space of the hydrogel network.[70,71] The farther apart the water molecules are located on the LPEI chain, the weaker is the bond that can form between them.[72] Hence, the LPEI melts gradually over a broad temperature range. The fact that the peak temperature from our hydrogel DSC scan was very high suggests a strong bonding between LPEI and some water molecules, i.e., those that are most strongly adsorbed on the polymer surface. I also conducted a second heating run on the sample after I held it isothermal at 200 ˚C for 1 minutes to ensure complete evaporation of the water molecules. Based on the TGA curve, the LPEI should not degrade at 200 ˚C. Therefore, any endothermic peak appearance on the second heating run can be regarded as the melting temperature of LPEI alone. As it can be seen in the inset in figure 8B, a small endothermic peak with peak temperature of 60.6˚C appeared. This result supports the argument that the first weight loss of 96.31 wt% was indeed from bounded

water in LPEI hydrogel network. The morphological transformation of LPEI from flat fiber bundles into pyramid-like structure is thus related to the LPEI-water interaction, whereas aggregate morphology observed at 6wt% could be the result of the overlapping polymers in the solution. Nevertheless, the critical gelation concentration to achieve pyramid-like structure was determined to be 3wt%.

3.3 Influence of Relative Humidity on Morphology of Coating Layer

In general, the microstructure of synthetic hydrogel such as LPEI is more reproducible compared to natural hydrogels (e.g. collagen and chitosan) because it has high purity, > 99 %; however, the microstructure can also depend on hydrogelation conditions in a subtle way. In this work, I observed that denser and smaller diameter of LPEI pillar structure can be tuned by the relative humidity of the surrounding air. I hypothesize that the relative humidity aids the fixation of water molecules in the LPEI hydrogel network.

3.3.1 Experimental details

The schematic diagram in figure 9 represents the sample preparation procedure for obtaining the X-ray diffraction pattern of LPEI under varying relative humidity conditions. The same procedure was performed for the coating process of the PU tubing. First, a closed chamber that contained saturated salt (e.g. $MgCl_2$ and NaOH) and DI water was allowed to equilibrate for at least a day before it was used. The relative humidity and temperature were measured immediately before the coating experiment was conducted using fisher scientific Traceable® relative humidity/temperature meter. It was noted that at 23 °C, relative humidity of the chamber that consists of DI water was 83%, with $MgCl_2$ it was 49%, and with NaOH it was 42%. Second, hot LPEI solution was prepared as described in section 2. The PU tubing was dipped into hot LPEI solution, withdrawn, and placed inside the chamber immediately. All samples were

analyzed the day after the experiment. LPEI crystal structure was analyzed by X-ray diffraction using the Rigaku Smartlab instrument with divergent beam BB (D/Tex) at room temperature. The test was scanned through a range of 2θ= 10- 60º, slit width of 10 mm, and the Kα line of a Cu target. The crystallinity was determined using Rigaku Smartlab PDXL ver.2.0 software.

3.3.2 Results and discussion

In section 3.2, we had demonstrated the significant influence of LPEI-water interaction to the morphological transformation of LPEI on the surface. We also demonstrated that adsorbed and perhaps absorbed water causes LPEI to have a broad melting temperature. Broad melting temperature could be an indication of impurities that causes defects in the crystal lattice. In such case, we expected that the melting temperature of LPEI to be less than the pure LPEI. Our data showed the otherwise. The melting peak shifted to higher temperature might be caused by new crystal structure formation of LPEI with water. [73] Therefore, water molecules play a role in stabilizing the crystal structure of LPEI.

A study by JJ. Yuan *et al.* had shown that LPEI with ~12.5 kDa exhibited very low critical gelation in neat water, which is 0.31%. [74] Given this fact and the hygroscopic nature of LPEI, our system, consisting of 3wt% of LPEI with 10 kDa, was expected to have the ability to take up water as it undergoes hydrogelation from the surrounding air. Hence, the process variable, such as relative humidity during the formation of hydrogel coating needs to be controlled.

Figure 9A depicts the surface morphology of LPEI coated PU tubing that was fabricated from different relative humidity conditions. We observed that the pyramids appear undeveloped under high relative humidity, as shown in figure 9A/RH 83%. The reason may be that LPEI absorbs more water under humid air, which prevents crystal formation. This is supported by the

X-ray diffraction of LPEI under RH of 83% where we can see that the pattern is dominated by two peaks, one at ~28° and the other at ~40°. They probably correspond to two kinds of amorphous packing, possibly of the gel. Probably water is in the gel, which is consistent with the TGA results. The crystallinity is calculated to be about 1.44%, which is quite low. As hydrogel is amorphous, the pyramid-like structure cannot hold its shape and thus appeared flat. The structure developed fully under ~50% RH (figure 9A/$MgCl_2$) and became denser and smaller at ~40% RH (figure 9A/NaOH). It was observed that the structure development is accompanied by increasing crystallinity of LPEI from 40.6 to 46.7%.

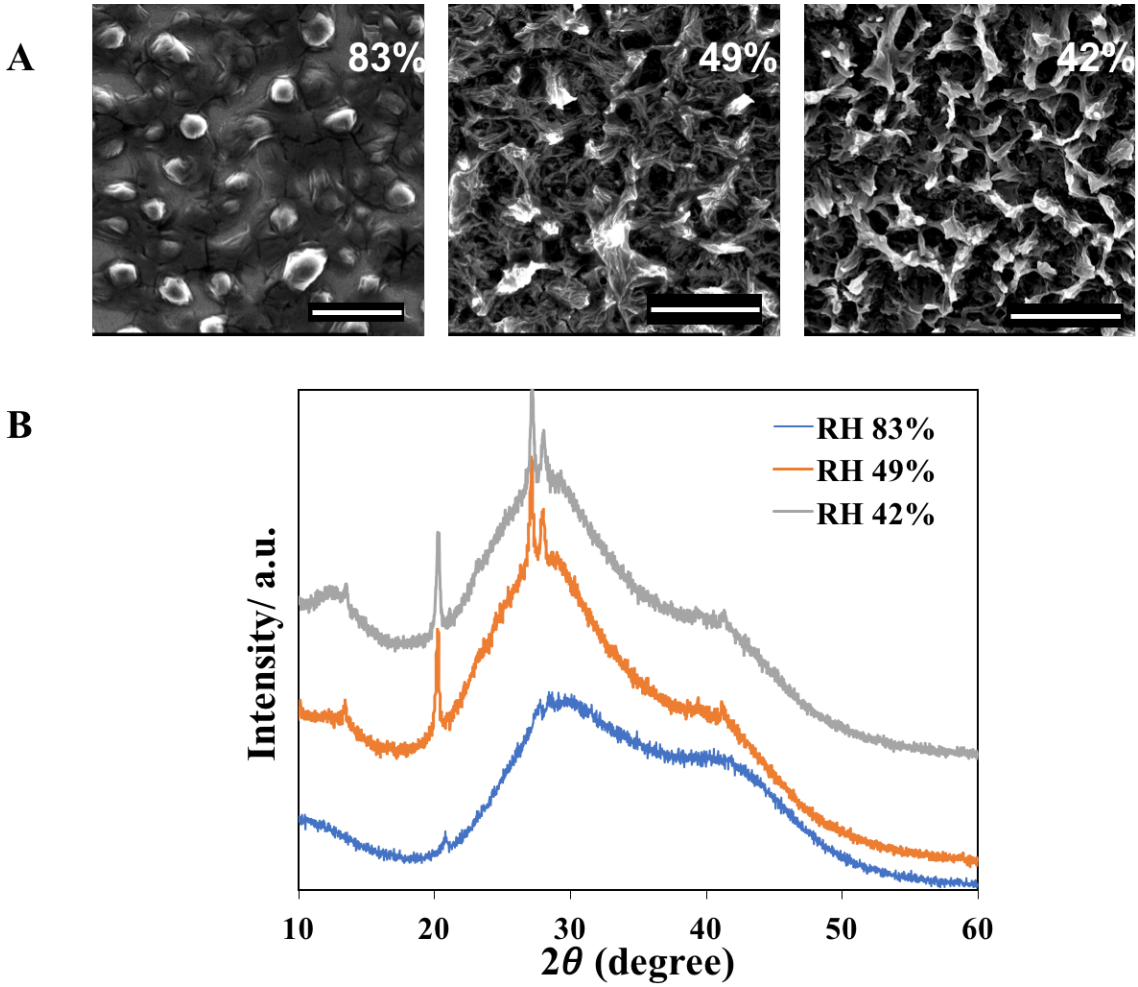

Figure 10. A) SEM images of LPEI coated PU surface evolution as a function of decreasing relative humidity from top left to top right. Scale bar 10 µm B) X-Ray diffraction pattern of LPEI hydrogel under different relative humidity conditions.

3.4 Chapter 3 Summary

This chapter discussed the influence of the deposition conditions of LPEI onto a surface, including the PU tubing surface. LPEI is a long chain of ethylenamine that interacts with water and depends on its pH strongly such that LPEI adopts several configurations in the solution. The effect of configurational changes of LPEI in the solution, subsequently, influences the wettability and adhesion of LPEI to a host surface.

In the acidic condition, amine acts as a base and attracts water molecules. The bound water molecules along LPEI chain increases LPEI dispersion in the aqueous solution. The adhesion between LPEI and the tubing surface is, thus, higher than its cohesive force. As a result, a thin coating of LPEI was obtained. In the basic condition, amine is a weaker base than the free hydroxyl groups. Amine groups are deprotonated and caused LPEI to collapse as aggregates (highly coiled chain) in the solution. Similarly, a thin coating of LPEI was obtained. I also discussed the influence of LPEI-water interaction on the morphology of the coating layer. The LPEI-water interaction increases as a result of increasing LPEI solution concentration. I found that the morphology of coating layer depends on the concentration of LPEI in the solution, and determined that the critical hydrogelation to result in a pyramid-like structure was 3wt%. Above this concentration, LPEI possesses an aggregate morphology. Another factor that can affect the morphology of LPEI coating layer is the relative humidity. Due to the hygroscopic nature of LPEI, it readily absorbs water from the surrounding air. At high humidity or when the amount of water in LPEI hydrogel is high, there are more amorphous regions in LPEI. As a result, I observed an undeveloped pyramid-like morphology. The pyramid-like structure loses its shape because the amorphous region softens the LPEI hydrogel structure. On the other hand, higher crystallinity leads to the formation of a defined pyramid-like structure.

4. Discussion

This thesis constitutes an investigation into the interaction between LPEI and the PU substrate, and the conditions that could be used to achieve a "pillar-like" structure. The aim is to develop a simple dip coating method of forming an antibacterial surface that can be translated into an industrial scale. We envision that the surface could be used in polymer-based medical devices as they are a common site for microbial infection. This thesis demonstrated the application of such surface morphology on catheter devices, specifically on urinary catheter devices. Although we had seen an increasing surface roughness on the surface of PU tubing as a result of pyramid-like structure, many steps remain to achieve the desired topographic surface, i.e. array of nanopillars, and to demonstrate that the surface could indeed be antimicrobial.

In chapter 2, I described the introduction of two functional groups responsible for the binding of LPEI onto the surface of the PU tubing. The two functional groups, isocyanate and ester, are formed as a result of oxygen plasma treatment. After having both functional groups exist concurrently after the plasma treatment, it is still rather unclear which functional groups will dominate the binding between LPEI and the PU tubing surface. Although the relative composition of the ester and isocyanate groups can be determined, it is difficult to do quantitative analysis by using FTIR data alone because the intensity is sensitive to the thickness of the sample material. Throughout this study, the coating thickness of LPEI has never been measured; thus, this quantitative analysis should be coupled with the coating thickness measurement such as profilometer.

Secondly, in section 3.1, it is evident that the configuration of LPEI macromolecules has significant influence on the surface morphology; however, we neglect the possibility of LPEI configurational changes as it adsorbs by the substrate. An analysis tool such as the Sum

Frequency Generation (SFG) spectroscopy can provide such understanding.[75] We believe that surface/polymer interactions play a role in the phase inversion (from liquid solution to solid) and the height of LPEI protrusion on the surface. Knowing how the polymers are arranged on the surface and what interactions that occurs in the interface, we could possibly have a better control in designing the LPEI microstructure.

Lastly, in urinary catheter, proper control of surface-polymer interface is required to avoid the detachment of the coating layer during catheter insertion. In another word, a strong bonding between the surface and polymer is important. Although our FTIR demonstrated that covalent bonding between the PU surface and LPEI was established, we found that the coating can be easily dewetted from the surface. In future work, we plan to coat LPEI on several different pretreated surfaces and evaluate the shear strength of the coating layer while also considering the effect of strong polymer adsorption on the surface to the morphology.

.

5. Future Work

Study of Linear Polyethylenimine Microstructure Surface on *Aspergillus fumigatus*

Studies have shown that cationic polymers are effective in killing and preventing the growth of gram-positive and gram-negative bacteria, and fungus.[76–79] Although it is still under debate, the killing mechanism of cationic polymers against microbes is proposed to originate from their high affinity to negatively-charged bacteria/fungal cell wall.[80] The binding between cationic polymer and the cell membrane causes reorganization of the membrane, thus forming pores that lead to bacterial and fungal cell lysis.[81] Thus, the efficacy of cationic polymers in combating microbial infection can be further enhanced by the cationic density.[78,82] Most antimicrobial activity studies of polycations are conducted in solution and not on a solid surface. When the polymer is tethered on the substrate, such as in our case where the LPEI is adhered and forms a film on the substrate, there is possibility of LPEI to lose their biocidal activity. In order to develop antimicrobial surfaces with LPEI as the building blocks, I investigated whether LPEI can kill microbial. The LPEI coated PU was tested against *Aspergilus fumigatus* spores because *A. fumigatus* is a common fungus that contaminates medical devices. Testing against this fungal strain may lead to promising data that can be applied to other strains.

In this work, I attempted to evaluate the antimicrobial effect of the LPEI coating. Even though I did obtain some interesting results, due to time limitations, I was not able to prove the results. Nevertheless, I include the results here as a record of my work, and to provide some information to those who might wish to follow up on this research.

5.1 Experimental details

The PU tubing surface was flattened down against glass slide and fixed using super glue. The flatten PU tubing was left a day to dry under ambient temperature before the coating process. Coating process was conducted using LPEI solution of 3wt%. As for the glass substrate, similar to PU tubing sample preparation, I surface treated the glass slide before coating process. The glass substrate was spin-coated with 0.5wt% poly (sodium 4-styrenesulfonate) aqueous solution (sigma Aldrich, BCBV0917) and annealed at 90 ˚C for an hour.[55] The glass was then dip-coated into hot LPEI solution of 3wt%, withdrawn immediately, and air dried under ambient temperature and humidity. To examine LPEI antimicrobial properties, samples were mounted at the bottom of a standard 6-well tissue culture plate with silicone glue to keep the samples submerged. Next, incubated *A. fumigatus* was suspended into 10 ml of 0.025 % PBS (phosphate-buffered saline broth) to loosen the hyphae of the fungi and separate the spores. The hyphae were then filtered out using a syringe and 3 filter paper sheets, leaving spores in the PBS. The spores were counted using a hemocytometer under light microscope. The dilution of about 10^5 spore/ml in RPMI (Roswell Park Memorial Institute) was pipetted into the culturing samples and monitored for 0, 8, and 16 hours. *A. fumigatus* live/dead imaging was taken using an inverted light microscope Cytation 5 cell reader by Biotek and quantified using ImageJ. Fixation of the fungi for SEM imaging was done by first immersing the sample under 2.5v% glutaldehyde in PBS solution. After 30 minutes, the excess solution was drained. The samples were then put into series of dehydration using 30%, 50%, 60%, 70%, 80%, 90%, 95%, and 100% of ethanol for 15 minutes each. The samples were dried under ambient temperature for at least a day before the SEM imaging. The fungi morphology was analyzed using Magellan field emission scanning electron microscopy (FESEM) with 5keV and 50pA.

5.2 Results and discussion

The phase images of *A. fumigatus* were captured after 0, 8, and 16 hours of culture. The results are shown in figure 10; uncoated PU was shown in row A and LPEI coated PU was shown in row B. Our experiment showed that there was no germination of the spores on the LPEI coated PU as we expected. On the uncoated PU substrate—our control—we did observe germination of *A. fumigatus,* leading to biofilm formation after 16 hours. This indicates that the LPEI coated surface either killed or prevented the growth of the spores. Unfortunately, we could not take any RFP and GFP images to analyze the live/dead spores. It is because the fluorescent light was scattered by the sample thickness, causing the substrate and spores to appear red in RFP image and green in GFP image. Moreover, poor condition of the sample reduces the contrast between the spores and the substrate, causing the quantification of fungi germination difficult to obtain. Hence, glass substrate was used.

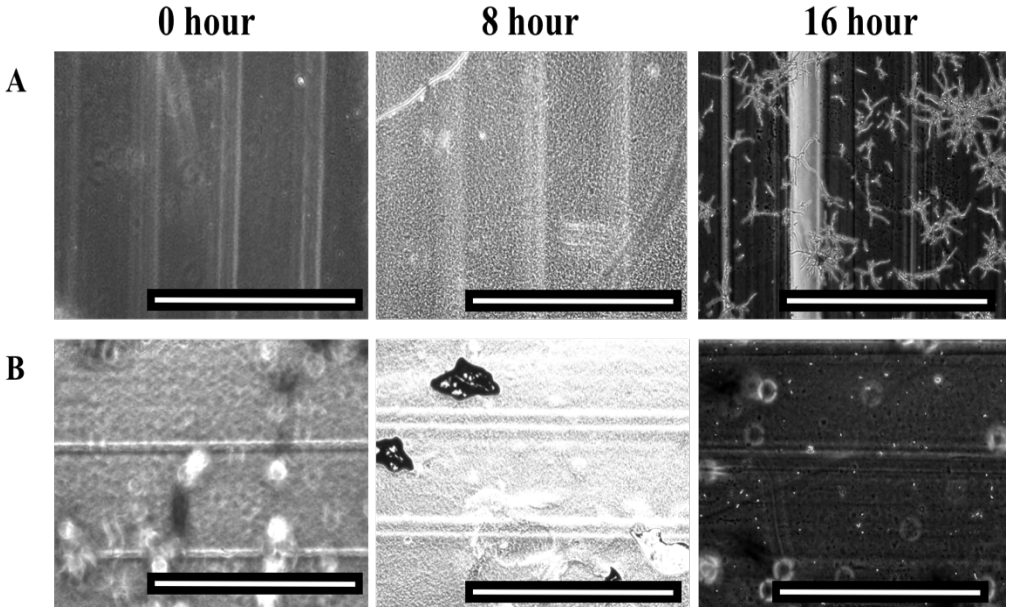

Figure 11. Optical microscope images of *Aspergillus fumigatus* growth on the plasma treated PU (A) and LPEI coated PU (B) from different time frame. The vertical line on the top images and horizontal line on the bottom images seen on PU substrates might be caused by the compressed force during the fixation of the PU tubing onto flat glass substrate. The ring artifact might cause by the entrapped air between the PU tubing and the flat glass substrate. Scale 1000μm.

Similar to PU substrate, we observed no *A. fumigatus* germination on the LPEI coated glass. On the other hand, the uncoated glass substrate showed germination of *A. fumigatus,* leading to biofilm formation after 16 hours. We further quantify the areal density coverage by

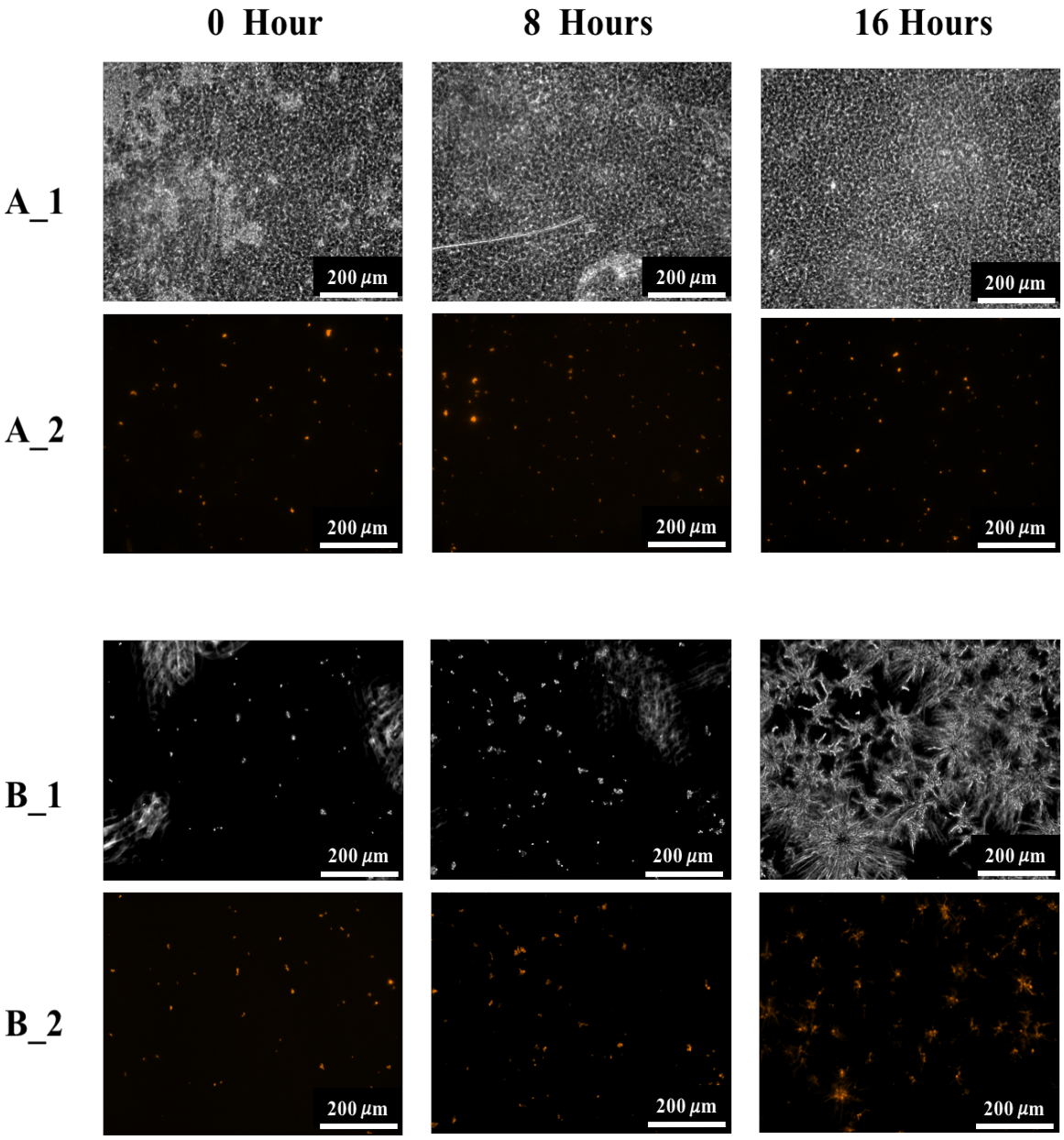

Figure 12. Optical microscope images of *Aspergillus fumigatus* growth on the glass substrate from different time frame. A) was phase image (A_1) and RFP (red fluorescent protein) image (A_2) of LPEI coated glass substrate. B) was phase image (B_1) and RFP image (B_2) of glass substrate. *A. fumigatus* spores on LPEI coated glass that is shown in row A_1was difficult to image as it was blocked by the LPEI microstructure.

fungi spores and the hyphae using ImageJ. While, increased of fungi germination on the uncoated glass was already seen after 8 hours of culturing and greatly increased after 16 hours, the LPEI coated glass showed no increased even after 16 hours. To study whether or not the surface morphology of LPEI coating contributes to the *A. fumigatus* impediment to growth, we took pictures of the sample SEM image. Unfortunately, there was no spore observed on the LPEI coated glass substrate. It was suspected that the spores were washed away during the fixation process. Although we expected that the different charges between LPEI and spores would increase the adherence of spores on the surface, it seems that the effect of LPEI surface structure in preventing the spores to adhere to the surface is more predominant. Another possible explanation is that the LPEI killed the spore, which subsequently cause the spore to die and detach from the surface. Either explanation requires further study.

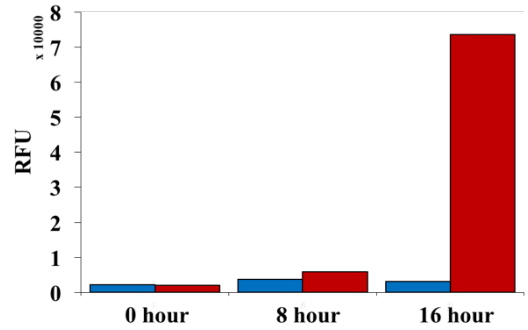

Figure 13. Relative fluorescence units count of *A. fumigatus* germination on the surface of uncoated glass (blue) and LPEI coated glass (red).

With this preliminary result, we had shown that LPEI could prevent the formation of *A. fumigatus* biofilm. The reason, however, still remains unclear. We observed that LPEI coating layer may have deteriorated during the fixation process, such that the surface morphology effect on the *A. fumigatus* development was not conclusive. Therefore, to ascertain that we can indeed cause LPEI to efficiently inhibit *A. fumigatus* growth, a study must be conducted on two surfaces composed of LPEI coating layer with and without pyramid-like morphology, the latter as a control. Furthermore, we need to utilize fluorescence microscopy to monitor the live/dead fungi

viability in real time to determine what mechanism is responsible for the fungi impediment to growth.

References

1. Regev-Shoshani, G., Ko, M., Miller, C. & Av-Gay, Y. Slow release of nitric oxide from charged catheters and its effect on biofilm formation by Escherichia coli. *Antimicrob. Agents Chemother.* **54,** 273–279 (2010).
2. Centers for Disease Control and Prevention. Urinary Tract Infection (Catheter-Associated Urinary Tract Infection [CAUTI] and Non-Catheter-Associated Urinary Tract Infection [UTI]) and Other Urinary System Infection [USI]) Events. *2016 NHSN Patient Saf. Compon. Man.* 1–16 (2016).
3. Fakih, M. G., Sanjay Saint, Milisa Manojlovich, Sarah Krein & Olmsted, R. AHRQ SAfety Program for for Reducing Reducing CAUTI in Hospitals. Toolkit for Reducing Catheter-Associated Urinary Tract Infections in Hospital Units : Implementation Guide Contents. *Agency Healthc. Res. Qual.* **3,** 6–26 (2013).
4. Nicolle, L. E. Catheter associated urinary tract infections. *Antimicrobial Resistance and Infection Control* **3,** (2014).
5. Singha, P., Locklin, J. & Handa, H. A review of the recent advances in antimicrobial coatings for urinary catheters. *Acta Biomaterialia* **50,** 20–40 (2017).
6. Tsuchida, T. *et al.* Relationship between catheter care and catheter-associated urinary tract infection at Japanese general hospitals: A prospective observational study. *Int. J. Nurs. Stud.* **45,** 352–361 (2008).
7. Donlan, R. M. & Costerton, J. W. Biofilms: Survival mechanisms of clinically relevant microorganisms. *Clinical Microbiology Reviews* **15,** 167–193 (2002).
8. Zhou, Z., Murdoch, W. J. & Shen, Y. A linear polyethylenimine (LPEI) drug conjugate with reversible charge to overcome multidrug resistance in cancer cells. *Polym. (United Kingdom)* **76,** 150–158 (2015).
9. Wang, W., Qu, X., Gray, A. I., Tetley, L. & Uchegbu, I. F. Self-assembly of cetyl linear polyethylenimine to give micelles, vesicles, and dense nanoparticles. *Macromolecules* **37,** 9114–9122 (2004).
10. Jung, H., Kim, S. A., Lee, E. & Mok, H. Linear polyethyleneimine-doxorubicin conjugate for pH-responsive synchronous delivery of drug and microRNA-34a. *Macromol. Res.* **23,** 449–456 (2015).
11. Tegos, G. P. *et al.* Protease-stable polycationic photosensitizer conjugates between polyethyleneimine and chlorin(e6) for broad-spectrum antimicrobial photoinactivation. *Antimicrob. Agents Chemother.* **50,** 1402–1410 (2006).
12. Fuchs, B. B., Tegos, G. P., Hamblin, M. R. & Mylonakis, E. Susceptibility of Cryptococcus neoformans to photodynamic inactivation is associated with cell wall integrity. *Antimicrob. Agents Chemother.* **51,** 2929–2936 (2007).
13. Lawrence, E. L. & Turner, I. G. Materials for urinary catheters: A review of their history and development in the UK. *Medical Engineering and Physics* **27,** 443–453 (2005).
14. Jacobsen, S. M., Stickler, D. J., Mobley, H. L. T. & Shirtliff, M. E. Complicated Catheter-Associated Urinary Tract Infections Due to Escherichia coli and Proteus mirabilis. *Clin. Microbiol. Rev.* **21,** 26–59 (2008).
15. Lim, K. *et al.* Development of a catheter functionalized by a polydopamine peptide coating with antimicrobial and antibiofilm properties. *Acta Biomater.* **15,** 127–138 (2015).
16. Donlan, R. M. Biofilms and device-associated infections. in *Emerging Infectious Diseases*

7, 277–281 (2001).
17. Platt, R., Polk, B. F., Murdock, B. & Rosner, B. Mortality associated with nosocomial urinary-tract infection. *N. Engl. J. Med.* **307,** 637–642 (1982).
18. Schaeffer, A. J. Catheter-associated bacteriuria. *Urol. Clin. North Am.* **13,** 735–47 (1986).
19. Thornton, G. F., Lytton, B. & Andriole, V. T. Bacteriuria During Indwelling Catheter Drainage: Effect of Constant Bladder Rinse. *JAMA J. Am. Med. Assoc.* **195,** 179–183 (1966).
20. Schaeffer, A. J. & Chmiel, J. Urethral meatal colonization in the pathogenesis of catheter-associated bacteriuria. *J. Urol.* **130,** 1096–9 (1983).
21. Daifuku, R. & Stamm, W. E. Association of Rectal and Urethral Colonization With Urinary Tract Infection in Patients With Indwelling Catheters. *JAMA J. Am. Med. Assoc.* **252,** 2028–2030 (1984).
22. Curtis Nickel, J., Grant, S. K., Lam, K., Olson, M. E. & William Costerton, J. Bacteriologically stressed animalmodel of new closed catheter drainage system with microbicidal outlet tube. *Urology* **38,** 280–289 (1991).
23. KHOURY, A. E., OLSON, M. E., LAM, K., NICKEL, J. C. & COSTERTON, J. W. Evaluation of the Retrograde Contamination Guard in a Bacteriologically Challenged Rabbit Model. *Br. J. Urol.* **63,** 384–388 (1989).
24. Broomfield, R. J., Morgan, S. D., Khan, A. & Stickler, D. J. Crystalline bacterial biofilm formation on urinary catheters by urease-producing urinary tract pathogens: A simple method of control. *J. Med. Microbiol.* **58,** 1367–1375 (2009).
25. Tsao, C. T. *et al.* Antibacterial activity and biocompatibility of a chitosan-gamma-poly(glutamic acid) polyelectrolyte complex hydrogel. *Carbohydr Res* **345,** 1774–1780 (2010).
26. Kalmodia, S., Molla, A. R. & Basu, B. In vitro cellular adhesion and antimicrobial property of SiO2-MgO-Al2O3-K2O-B2O3-F glass ceramic. *J. Mater. Sci. Mater. Med.* **21,** 1297–1309 (2010).
27. Roy, S. & Das, P. K. Antibacterial hydrogels of amino acid-based cationic amphiphiles. *Biotechnol. Bioeng.* **100,** 756–764 (2008).
28. Gao, G. *et al.* Antibacterial surfaces based on polymer brushes: Investigation on the influence of brush properties on antimicrobial peptide immobilization and antimicrobial activity. *Biomacromolecules* **12,** 3715–3727 (2011).
29. Glinel, K., Jonas, A. M., Jouenne, T., Galas, L. & Huck, W. T. S. Antibacterial and Antifouling Polymer Brushes Incorporating Antimicrobial Peptide Antibacterial and Antifouling Polymer Brushes Incorporating Antimicrobial Peptide. *Bioconjug. Chem.* **20,** 71–77 (2009).
30. Loo, C. Y. *et al.* Superhydrophobic, nanotextured polyvinyl chloride films for delaying Pseudomonas aeruginosa attachment to intubation tubes and medical plastics. *Acta Biomater.* **8,** 1881–1890 (2012).
31. Mi, L. & Jiang, S. Integrated antimicrobial and nonfouling zwitterionic polymers. *Angewandte Chemie - International Edition* **53,** 1746–1754 (2014).
32. Pickard, R. *et al.* Antimicrobial catheters for reduction of symptomatic urinary tract infection in adults requiring short-term catheterisation in hospital: A multicentre randomised controlled trial. *Lancet* **380,** 1927–1935 (2012).
33. Lederer, J. W., Jarvis, W. R., Thomas, L. & Ritter, J. Multicenter cohort study to assess the impact of a silver-alloy and hydrogel-coated urinary catheter on symptomatic catheter-

associated urinary tract infections. *J. Wound, Ostomy Cont. Nurs.* **41,** 473–480 (2014).
34. Gould, C. V, Umscheid, C. A., Agarwal, R. K., Kuntz, G. & Pegues, D. A. Guideline for Prevention of Catheter - Associated Urinary Tract Infections 2009. *Healthc. Infect. Control Pract. Advis. Comm.* 1–61 (2017). doi:10.1086/651091
35. Jelenko, C. Silver Nitrate Resistant E. coli: Report of Case. *Ann. Surg.* **170,** 296–299 (1969).
36. Graves, J. L. *et al.* Rapid evolution of silver nanoparticle resistance in Escherichia coli. *Front. Genet.* **5,** (2015).
37. Campoccia, D., Montanaro, L. & Arciola, C. R. A review of the biomaterials technologies for infection-resistant surfaces. *Biomaterials* **34,** 8533–8554 (2013).
38. Renner, L. D. & Weibel, D. B. Physicochemical regulation of biofilm formation. *MRS Bulletin* **36,** 347–355 (2011).
39. Parreira, P. *et al.* Effect of surface chemistry on bacterial adhesion, viability, and morphology. *J. Biomed. Mater. Res. - Part A* **99 A,** 344–353 (2011).
40. Tegoulia, V. A. & Cooper, S. L. Staphylococcus aureus adhesion to self-assembled monolayers: effect of surface chemistry and fibrinogen presence. *Colloids and Surfaces B: Biointerfaces* **24,** 217–228 (2002).
41. Wiencek, K. M. & Fletcher, M. Bacterial adhesion to hydroxyl- and methyl-terminated alkanethiol self- assembled monolayers. *J. Bacteriol.* **177,** 1959–1966 (1995).
42. Van Der Mei, H. C., Bos, R. & Busscher, H. J. A reference guide to microbial cell surface hydrophobicity based on contact angles. *Colloids and Surfaces B: Biointerfaces* **11,** 213–221 (1998).
43. Shanks, R. M. *et al.* Heparin stimulates Staphylococcus aureus biofilm formation. *Infect Immun* **73,** 4596–4606 (2005).
44. Gottenbos, B., Grijpma, D. W., van der Mei, H. C., Feijen, J. & Busscher, H. J. Antimicrobial effects of positively charged surfaces on adhering Gram-positive and Gram-negative bacteria. *J. Antimicrob. Chemother.* **48,** 7–13 (2001).
45. Sun, X., Cao, Z., Porteous, N. & Sun, Y. An N-halamine-based rechargeable antimicrobial and biofilm controlling polyurethane. *Acta Biomater.* **8,** 1498–1506 (2012).
46. Terada, A., Okuyama, K., Nishikawa, M., Tsuneda, S. & Hosomi, M. The effect of surface charge property on Escherichia coli initial adhesion and subsequent biofilm formation. *Biotechnol. Bioeng.* **109,** 1745–1754 (2012).
47. van Loosdrecht, M. C., Lyklema, J., Norde, W. & Zehnder, A. J. Influence of interfaces on microbial activity. *Microbiol. Rev.* **54,** 75–87 (1990).
48. Koo, H., Allan, R. N., Howlin, R. P., Stoodley, P. & Hall-Stoodley, L. Targeting microbial biofilms: Current and prospective therapeutic strategies. *Nature Reviews Microbiology* **15,** 740–755 (2017).
49. May, R. M. *et al.* An engineered micropattern to reduce bacterial colonization, platelet adhesion and fibrin sheath formation for improved biocompatibility of central venous catheters. *Clin. Transl. Med.* **4,** 9 (2015).
50. Xu, L. C. & Siedlecki, C. A. Staphylococcus epidermidis adhesion on hydrophobic and hydrophilic textured biomaterial surfaces. *Biomed. Mater.* **9,** (2014).
51. Tripathy, A., Sen, P., Su, B. & Briscoe, W. H. Natural and bioinspired nanostructured bactericidal surfaces. *Advances in Colloid and Interface Science* **248,** 85–104 (2017).
52. Ivanova, E. P. *et al.* Bactericidal activity of black silicon. *Nat. Commun.* **4,** (2013).
53. Dickson, M. N., Liang, E. I., Rodriguez, L. A., Vollereaux, N. & Yee, A. F.

Nanopatterned polymer surfaces with bactericidal properties. *Biointerphases* **10,** 021010 (2015).
54. Biswas, A. *et al.* Advances in top-down and bottom-up surface nanofabrication: Techniques, applications & future prospects. *Advances in Colloid and Interface Science* **170,** 2–27 (2012).
55. Yuan, J. J., Kimitsuka, N. & Jin, R. H. Bioinspired synthesis of a soft-nanofilament-based coating consisting of polysilsesquioxanes/polyamine and its divergent surface control. *ACS Appl. Mater. Interfaces* **5,** 3126–3133 (2013).
56. Jin, R. H. & Yuan, J. J. Biomimetically controlled formation of nanotextured silica/Titania films on arbitrary substrates and their tunable surface function. *Adv. Mater.* **21,** (2009).
57. Coffman, E. A., Melechko, A. V., Allison, D. P., Simpson, M. L. & Doktycz, M. J. Surface patterning of silica nanostructures using bio-inspired templates and directed synthesis. *Langmuir* **20,** 8431–8436 (2004).
58. Carmona-Ribeiro, A. M. & de Melo Carrasco, L. D. Cationic antimicrobial polymers and their assemblies. *International Journal of Molecular Sciences* **14,** 9906–9946 (2013).
59. Breunig, M. *et al.* Gene delivery with low molecular weight linear polyethylenimines. *J. Gene Med.* **7,** 1287–1298 (2005).
60. Neu, M., Fischer, D. & Kissel, T. Recent advances in rational gene transfer vector design based on poly(ethylene imine) and its derivatives. *Journal of Gene Medicine* **7,** 992–1009 (2005).
61. Yeaman, M. R. Mechanisms of Antimicrobial Peptide Action and Resistance. *Pharmacol. Rev.* **55,** 27–55 (2003).
62. Thoma, L. M., Boles, B. R. & Kuroda, K. Cationic methacrylate polymers as topical antimicrobial agents against staphylococcus aureus nasal colonization. *Biomacromolecules* **15,** 2933–2943 (2014).
63. Blessing, T., Kursa, M., Holzhauser, R., Kircheis, R. & Wagner, E. Different strategies for formation of PEGylated EGF-conjugated PEI/DNA complexes for targeted gene delivery. *Bioconjug. Chem.* **12,** 529–537 (2001).
64. Zandén, C. *et al.* Surface characterisation of oxygen plasma treated electrospun polyurethane fibres and their interaction with red blood cells. *Eur. Polym. J.* **48,** 472–482 (2012).
65. Mohrig, J. R., Hammond, C. N. & Schatz, P. F. Infrared Spectroscopy. in *Techniques in Organic Chemistry* 277–310 (W. H. Freeman and Company, 2010).
66. Douglas, J. F. How Does Surface Roughness Affect Polymer-Surface Interactions? *Macromolecules* **22,** 3707–3716 (1989).
67. Choudhury, C. K. & Roy, S. Structural and dynamical properties of polyethylenimine in explicit water at different protonation states: a molecular dynamics study. *Soft Matter* **9,** 2269 (2013).
68. Chandler, D. Interfaces and the driving force of hydrophobic assembly. *Nature* **437,** 640–647 (2005).
69. Rao, M. V. S. Viscosity of dilute to moderately concentrated polymer solutions. *Polymer (Guildf).* **34,** 592–596 (1993).
70. Capitani, D., Crescenzi, V., De Angelis, A. A. & Segre, A. L. Water in hydrogels. An NMR study of water/polymer interactions in weakly cross-linked chitosan networks. *Macromolecules* **34,** 4136–4144 (2001).
71. Liu, W. G. & Yao, K. De. What causes the unfrozen water in polymers: Hydrogen bonds

between water and polymer chains? *Polymer (Guildf).* **42,** 3943–3947 (2001).
72. Guan, L., Xu, H. & Huang, D. The investigation on states of water in different hydrophilic polymers by DSC and FTIR. *J. Polym. Res.* **18,** 681–689 (2011).
73. Hashida, T., Tashiro, K. & Inaki, Y. Crystallization of poly(ethylene imine) amorphous sample in water vapor atmosphere. *Polymer (Guildf).* **44,** 1721–1724 (2003).
74. Yuan, J. J. & Jin, R. H. Fibrous crystalline hydrogels formed from polymers possessing a linear poly(ethyleneimine) backbone. *Langmuir* **21,** 3136–3145 (2005).
75. Somorjai, G. A. & Mujumdar, A. S. Introduction to surface chemistry and catalysis. *Dry. Technol.* **13,** 507–508 (1995).
76. Liu, R. *et al.* Nylon-3 polymers with selective antifungal activity. *J. Am. Chem. Soc.* **135,** 5270–5273 (2013).
77. Liu, R. *et al.* Nylon-3 polymers active against drug-resistant candida albicans biofilms. *J. Am. Chem. Soc.* **137,** 2183–2186 (2015).
78. He, Y., Heine, E., Keusgen, N., Keul, H. & Möller, M. Synthesis and characterization of amphiphilic monodisperse compounds and poly(ethylene imine)s: Influence of their microstructures on the antimicrobial properties. *Biomacromolecules* **13,** 612–623 (2012).
79. Tejero, R. *et al.* Tailoring macromolecular structure of cationic polymers towards efficient contact active antimicrobial surfaces. *Polymers (Basel).* **10,** (2018).
80. Gilbert, P. & Moore, L. E. Cationic antiseptics: Diversity of action under a common epithet. *Journal of Applied Microbiology* **99,** 703–715 (2005).
81. Ganewatta, M. S. & Tang, C. Controlling macromolecular structures towards effective antimicrobial polymers. *Polym. (United Kingdom)* **63,** A1–A29 (2015).
82. Punia, A., He, E., Lee, K., Banerjee, P. & Yang, N.-L. Cationic amphiphilic non-hemolytic polyacrylates with superior antibacterial activity. *Chem. Commun.* **50,** 7071 (2014).